Gene Expression, Vol. 15, pp. 183–198
Printed in the USA.

1052-2166/12 $90.00 + .00
DOI: http://dx.doi.org/10.3727/105221612X13372578119698
E-ISSN 1555-3884
www.cognizantcommunication.com

Distribution of Histone3 Lysine 4 Trimethylation at T3-Responsive Loci in the Heart During Reversible Changes in Gene Expression

KUMAR PANDYA,*[1] TAKAHIDE KOHRO,†[1] IMARI MIMURA,† MIKA KOBAYASHI,† YOUICHIRO WADA,† TATSUHIKO KODAMA,† AND OLIVER SMITHIES*

**Department of Pathology and Laboratory Medicine, University of North Carolina at Chapel Hill, Chapel Hill, NC, USA*
†Department of Molecular Biology and Medicine, The Research Center for Advanced Science and Technology, The University of Tokyo, Tokyo, Japan

Expression in the adult heart of a number of cardiac genes, including the two genes comprising the cardiac myosin heavy chain locus (Myh), is controlled by thyroid hormone (T3) levels, but there is minimal information concerning the epigenetic status of the genes when their expressions change. We fed mice normal chow or a propyl thio uracil (PTU, an inhibitor of T3 production) diet for 6 weeks, or the PTU diet for 6 weeks followed by normal chow for a further 2 weeks. Heart ventricles from these groups were then used for ChIP-seq analyses with an antibody to H3K4me3, a well-documented epigenetic marker of gene activation. The resulting data show that, at the Myh7 locus, H3K4me3 modifications are induced primarily at 5′ transcribed region in parallel with increased expression of beta myosin heavy chain (MHC). At the Myh6 locus, decreases in H3K4me3 modifications occurred at the promoter and 5′ transcribed region. Extensive H3K4me3 modifications also occurred at the intergenic region between the two Myh genes, which extended into the 3′ transcribed region of Myh7. The PTU-induced changes in H3K4me3 levels are, for the most part, reversible but are not invariably complete. We found full restoration of Myh6 gene expression upon PTU withdrawal; however, the H3K4me3 pattern was only partially restored at Myh6, suggesting that full reexpression of Myh6 does not require that the H3K4me3 modifications return fully to the untreated conditions. Together, our data show that the H3K4me3 modification is an epigenetic marker closely associated with changes in Myh gene expression.

Key words: Myosin heavy chain; Epigenetic; ChIP-seq; Thyroid hormone; Heart; Histone methylation

INTRODUCTION

The amino-terminal tails of histones are the target of multiple posttranslational modifications: acetylation, methylation, phosphorylation, and ubiquitination (14,17). Multiple studies have revealed predictive correlations between histone modifications and gene expression (6,18). Trimethylation of lysine residue at position 4 of histone 3 (H3K4me3) is one such modification that is highly correlated with active gene

[1]Co-first authors.

Address correspondence to Oliver Smithies, D.Phil., Department of Pathology and Laboratory Medicine, University of North Carolina at Chapel Hill, 701 Brinkhous Bullit Building, Chapel Hill, NC 27599-7525, USA. Tel: +1-919-966-6912; Fax: +1-919-966-8800; E-mail: jenny_langenbach@med.unc.edu *or* Youichiro Wada, M.D., Ph.D., Laboratory of Systems Biology and Medicine, Research Center for Advanced Science and Technology, University of Tokyo, 4th building Room 310, 4-6-1 Komaba, Meguro-ku, Tokyo 153-8904, Japan. Tel: +81-3-5452-5117; Fax: +81-3-5452-5117; E-mail: ywada-tky@umin.ac.jp

expression (24). Genome-wide studies have found this modification to be present frequently within the promoters of genes that are actively transcribed, and it is now considered to be a well-conserved marker of gene activation (16,29). Several components of the transcriptional machinery contain domains (such as PHD, chromo, bromo, MCT, and Tudor) that can recognize H3K4me3 (12). The H3K4me3 modification may serve as a general means of recruiting transcriptional machinery. Determining how the distribution of H3K4me3 modification changes in response to defined stimuli is critical to understanding how genes are regulated.

Thyroid hormone (T3) is a fat-soluble hormone produced by the thyroid gland, which is released into the circulation and plays critical roles in differentiation, growth, and metabolism (30). The effects of T3 on heart function are well documented, and various studies have identified multiple genes whose expression levels are responsive to T3 levels, including the two cardiac myosin heavy chain (Myh) genes, sarcoplasmic reticulum Ca^{2+} ATPase, and several membrane-bound sodium and potassium channels (3,11, 21). T3 binds to the thyroid hormone receptor (THR)—a member of nonsteroidal nuclear hormone receptor family—and exerts its effects by either inducing or silencing the expression of target genes (2). THR binds to its recognition site independently of T3, although the presence or absence of T3 controls whether THR is a transcriptional activator or transcriptional repressor.

The two genes of the Myh locus, Myh6 and Myh7, are some of the most T3-responsive genes in the heart. They code for the developmental stage-specific isoforms of the myosin heavy chain component of the sarcomere—the fundamental unit of contraction of the muscle cell. Myh7 (beta-MHC) is expressed at high levels during the fetal stage in the mouse ventricle, during which Myh6 (alpha-MHC) is expressed at very low levels. Immediately after birth, in response to a surge in the circulating levels of T3, the expression of Myh7 is silenced and that of Myh6 increases so that alpha-MHC becomes the predominant isoform of myosin heavy chain. Under conditions of hypothyroidism, heart failure, and cardiac hypertrophy, there is a reversal in the expression pattern of these two genes: Myh7 expression is induced and Myh6 is silenced.

The degree to which T3-mediated changes in Myh gene expression are associated with changes in H3K4me3 levels is of considerable interest, as is the degree to which H3K4me3 modification is reversible during reversible changes in gene expression. Previous

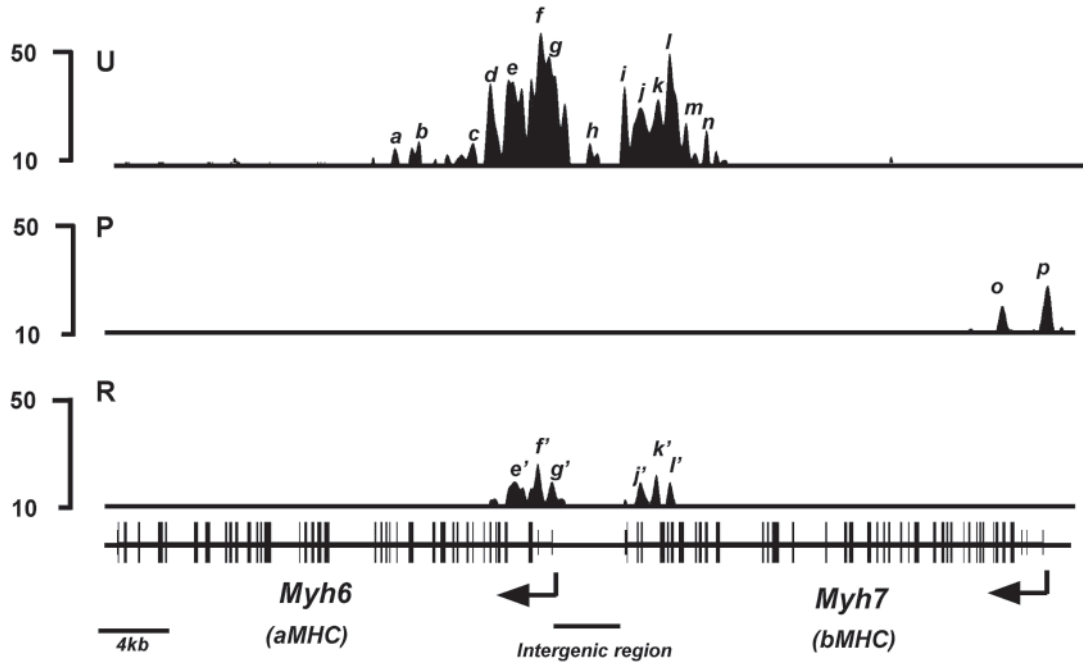

Figure 1. H3K4me3 enrichment profile of Myh loci. H3K4me3 signal intensities are shown on the *y*-axis and schematic of the Myh locus shown on the *x*-axis. Animals were fed either regular chow (untreated), PTU diet for 6 weeks (PTU), or PTU diet for 6 weeks followed by regular chow for a further 2 weeks (reversal), and hearts were isolated for analyses. ChIP-seq analyses were conducted using anti-H3K4me3 antibody from chromatin isolated from untreated (U, top panel), PTU-treated (P, middle panel), or reversal (R, bottom panel) animals. H3K4me3 signals are illustrated from the Integrated Genome Browser interface. Exons are represented as closed boxes; bent arrows show the transcriptional start site (TSS) and direction of transcription. Intergenic region between the two Myh genes is identified with a horizontal bar. Individual peaks are identified by letters in italics. Scale bar for the locus is shown at the bottom left.

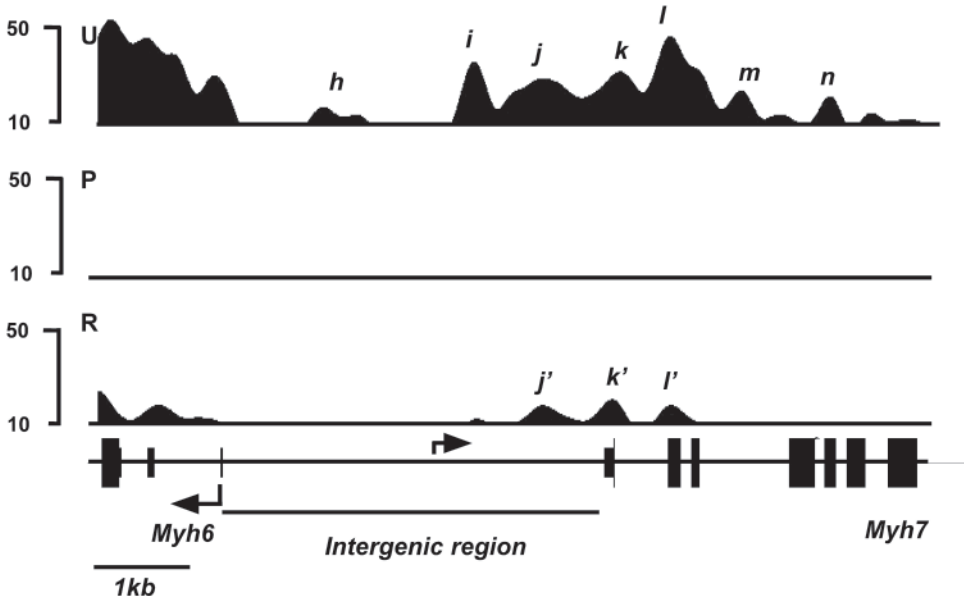

Figure 2. H3K4me3 enrichment profile of Myh intergenic region. H3K4me3 signal intensities are shown on the *y*-axis and schematic of the locus shown on the *x*-axis. Animals were fed either regular chow (untreated), PTU diet for 6 weeks (PTU), or PTU diet for 6 weeks followed by regular chow for a further 2 weeks (reversal), and hearts were isolated for analyses. ChIP-seq analyses were conducted using anti-H3K4me3 antibody from chromatin isolated from Untreated (U, top panel), PTU-treated (P, middle panel), or reversal (R, bottom panel) animals. Exons are represented as closed boxes; bent arrows show the transcriptional start site (TSS) and direction of transcription. Intergenic region between the two Myh genes is identified with a horizontal bar. Individual peaks are identified by letters in italics. Scale bar for the locus is shown at the bottom left.

work conducted by us using a chromatin immunoprecipitation (ChIP)-qPCR assay demonstrated that this modification occurred at the promoter of Myh6 but not Myh7 (20). However, this previous investigation did not interrogate regions outside the promoters. Consequently, in this report, we have comprehensively investigated the changes in H3K4me3 levels across the entire Myh loci using the more powerful ChIP-seq procedure. This combines ChIP with deep sequencing, which results in a sensitive and unbiased way of investigating the H3K4me3 status within individual genes across the whole genome. Here, we show that the H3K4me3 modification occurs at multiple regions within the Myh locus, including the 5′ transcribed portion of Myh7. We also show H3K4me3 modification at an intergenic region that

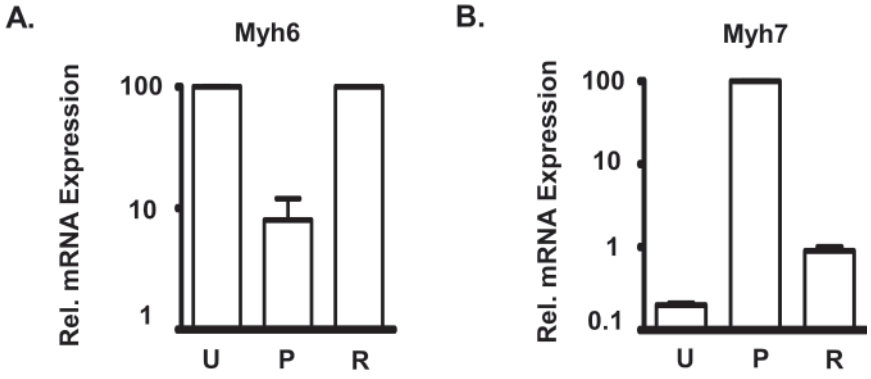

Figure 3. Reversible changes in mRNA expression levels of Myh genes in response to PTU treatment. Comparisons of mRNA expressions for Myh6 (A) and Myh7 (B) from hearts of untreated (U), PTU-treated (P), and reversal (R) groups. The mean for untreated group (for Myh6) or PTU-treated group (for Myh7) was set at 100, and the values for the other groups are relative to this value (relative expression). Animals were fed either regular chow (U), PTU diet for 6 weeks (P), or PTU diet for 6 weeks followed by regular chow for a further 2 weeks (R), and hearts were isolated for analyses. Quantitative gene expressions were determined by Taqman real-time PCR. Individual values ± SD are: Myh6 (U): 100 ± 4; Myh6 (P): 8 ± 4; Myh6 (R): 115 ± 8; Myh7 (U): 0.2 ± 0.01; Myh7(P): 100 ± 5.7; Myh7(R): 0.9 ± 0.1.

TABLE 1
T3-RESPONSIVE HEART GENES

Actg2	Actin, gamma 2, smooth muscle, enteric
Aldoc	Aldose C, fructose-bisphosphate
Ankrd1	Ankyrin repeat domain 1 protein
Atp1b1	Sodium/Potassium-transporting ATPase subunit beta-1
Atp2a2	ATPase, Ca^{2+} transporting, cardiac muscle, slow twitch2
Atp5a1	Mitochondrial H^{+}-ATPase synthase alpha subunit
Brp44l	Brain protein 44-like
Bpnt1	3′(2′),5′-bisphosphate nucleotidase
Cacna1c	Ca^{2+} channel
Ctrb1	Chymotrypsin B
Cycs	Cytochrome C
Cx3c	Chemokin Cx3c
Dab2	DOC-2 p82 isoform
Dcn	Decorin
Fabp3	Adipocyte lipid-binding protein
Fbp1	Fructose 1,6-biphosphate
Fxyd5	FXYD domain-containing ion transport regulator-1
Hr	Hairless
Itga7	Alpha7A integrin
Kcna5	Potassium channel a5
Kcnb1	Potassium channel b1
Kcnd2	Potassium channel d2
Kcne1	Potassium channel e1
Kcnj11	Sulfonyl urea receptor
Kcnk2	Potassium channel k2
Kcnq1	Potassium channel q1
Mdh1	Malate dehydrogenase-like enzyme
Mgp	Matrix G1a protein
Myh6	Cardiac myosin heavy chain, alpha
Myh7	Cardiac nyosin heavy chain, beta
Myh13	Myosin, heavy chian polypeptide, 13, skeletal muscle
Nppa	Natriuretic peptide precursor A
Nppb	Brain natriuretic factor
Nrp1	Neuropilin
Pln	Phospholamban
Rgs4	Regulator of G-protein signaling 4
S100a4	S100 calcium binding protein A4
Slc8a1	Ca^{2+} regulatory channel
Slc2a4	Glucose transporter 4, insulin responsive
Tmprss13	Protease, serine, 11 (IgF binding)
Tnp2	Transition protein 2
Wfdc8	WAP four-disulfide core domain 8

Putative T3-resposnive genes whose expression was previously shown to change >2× in response to changes in T3 levels (1,15).

coincides with a previously demonstrated antisense promoter. Finally, we show that the H3K4me3 modification occurs at many regions within the genome and that it is at least partially reversible in response to reversible changes in T3.

MATERIALS AND METHODS

Animals

Animals used in this study were 4-month-old 129/Svev. Animals were fed an iodine-deficient diet containing 0.15% PTU (Harlan Teklad, TD. 97061, Rx257896) for 6 weeks, and then either sacrificed (PTU group) or fed normal chow for another 2 weeks (reversal). Control mice were fed normal chow. The mice were maintained in a facility accredited by the Association for the Assessment and Accreditation of Laboratory Animal Care International according to Institutional Animal Care and Use Committee-approved guidelines.

Organ Preparation for Chromatin Immunoprecipitation (ChIP)

Hearts were excised immediately after euthanasia and cut into two pieces to remove residual blood. Then they were washed in PBS and snap frozen in liquid nitrogen. Hearts were treated with 1% formaldehdye for 20 min, followed by treatment with glycine to quench fixation. Nuclear extracts were prepared by crushing with Cryo-Press CP-100 (Microtech Nichion, Co. Ltd, Japan), as described previously (27). Briefly, approximately 300 mg of frozen heart tissue was physically crushed with Cryo-Press for 1 min four times, changing direction of liquid nitrogen-cooled sample container. Frozen powder of heart was immediately suspended in 2 ml of SDS lysis buffer (10 mM Tris-HCl, pH 8.0, 150 mM NaCl, 1% SDS, 1 mM EDTA). Cell suspension including DNA–protein complex was applied to fragmentation using Sonifier (Branson); 10 min for high-speed sequencer. Samples were diluted by 2 ml of ChIP dilution buffer (20 mM Tris-HCl, pH 8.0, 150 mM NaCl, 1 mM EDTA, 1% Triton X-100) and applied to chromatin immunoprecipitation. Detailed experimental procedure for chromatin immunoprecipitation followed with high-speed sequencer was modified as described elsewhere (28). H3K4me3-bound genomic DNA was isolated from whole cell lysate using a mouse monoclonal antibody [16H10, a gift of Dr. Hiroshi Kimura (13)], in combination with magnetic beads (Dynal/Invitrogen). Prepared DNA was quantified using Qubit (Invitrogen) and more than 10 ng of DNA was processed as described below.

ChIP-seq Sample Preparation and Analysis

All protocols for Illumina/Solexa sequence preparation, sequencing, and quality control were provided by Illumina (http://www.illumina.com/pages.ilmn?ID=203) (25).

Microarray Analyses

Ventricles of the hearts from the different conditions were surgically isolated, frozen in liquid nitrogen, and RNA isolated. Total RNA was submitted for microarray analyses as previously described (27).

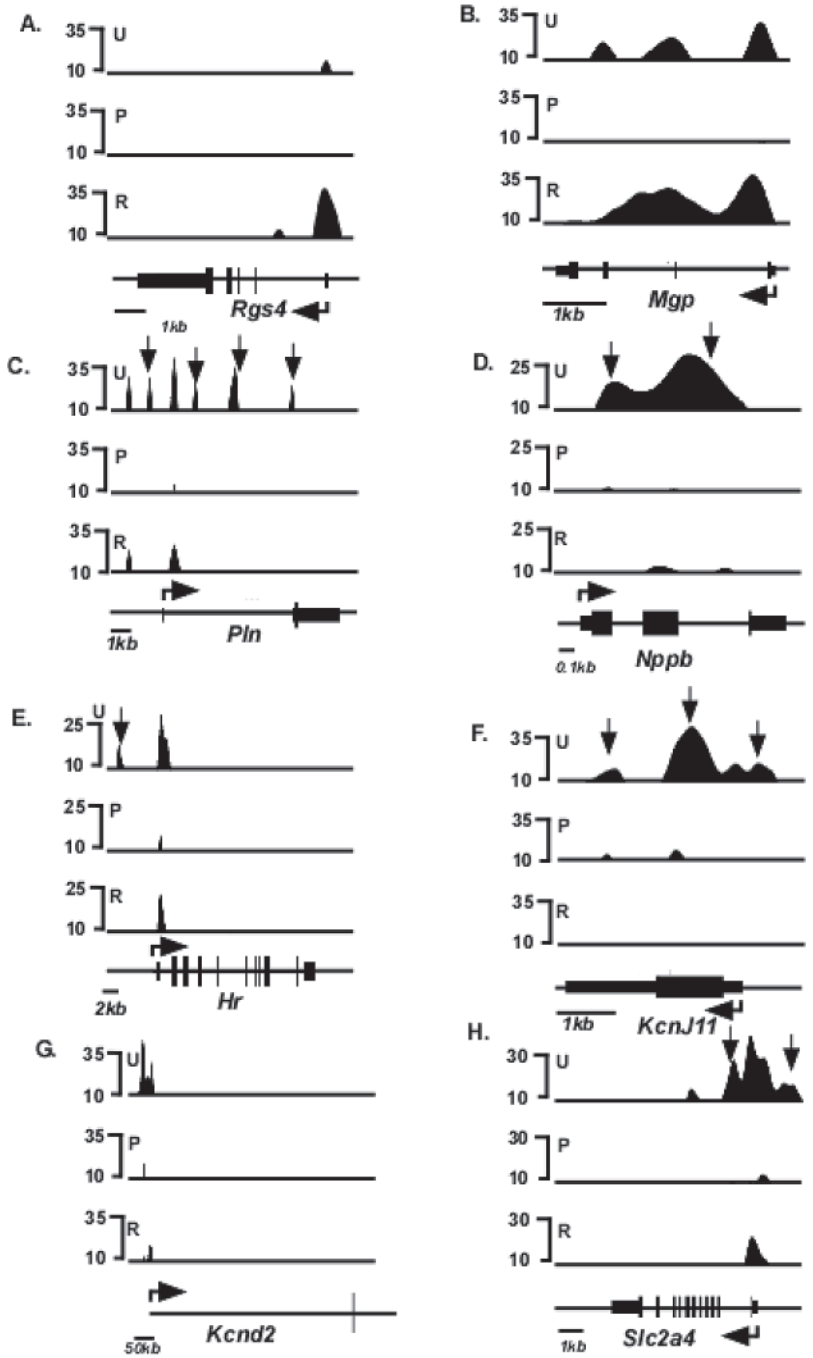

Figure 4. Schematic of H3K4me3 enrichment profile of T3-responsive genes that respond to PTU treatment. Relative H3K4me3 signal intensities are shown on the *y*-axis and schematics of individual gene loci shown on the *x*-axis. ChIP-seq analyses were conducted using anti-H3K4me3 antibody from chromatin isolated from untreated (U, top panel), PTU-treated (P, middle panel), or reversal (R, bottom panel) animals. Exons are represented as closed boxes; bent arrows show the transcriptional start site (TSS) and direction of transcription. Quantitation of these data is presented in Tables 2 and 3. Vertical arrows in (D, F, G) (Hr, Kcnj11, and Pln) identify H3K4me3 peaks that are present in untreated (U) but not in reversal (R) conditions, depicting incomplete reversal. Genes whose loci showed >2× or <2× changes in H3K4me3 levels in response to PTU were considered PTU responsive. Scale bars for each locus are shown at the bottom left of each panel.

RESULTS

ChIP-seq Analyses for H3K4me3 Occupancy

The distribution of the H3K4me3 modification was determined by chromatin immunoprecipitation/high throughput sequencing (ChIP-seq) analyses on heart samples, which enables analysis of H3K4me3 distribution across the whole genome. We used cardiac ventricles from 4-month-old 129/Svev mice and conducted ChIP-seq assays with an antibody specific for

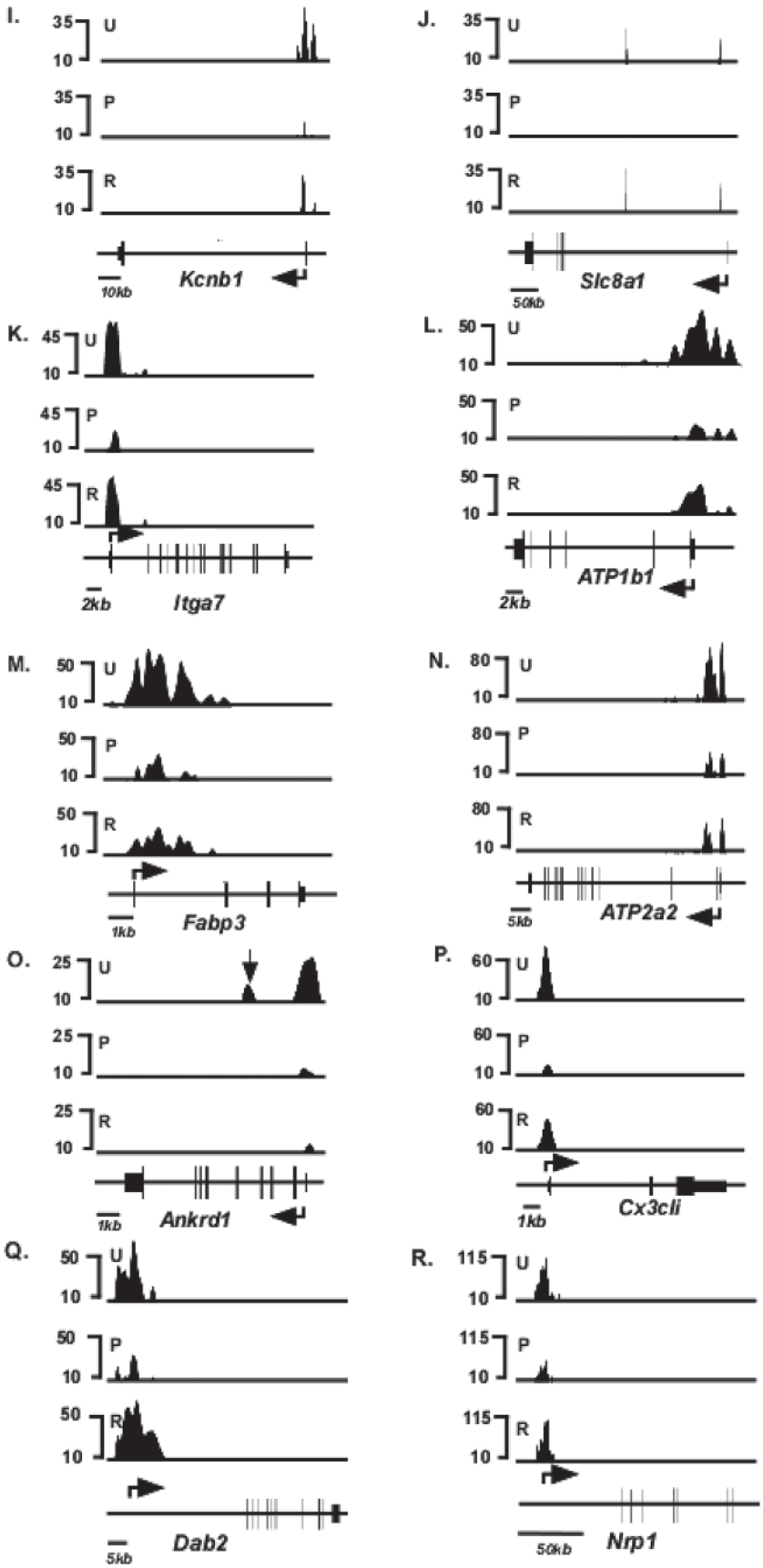

Figure 4. Continued.

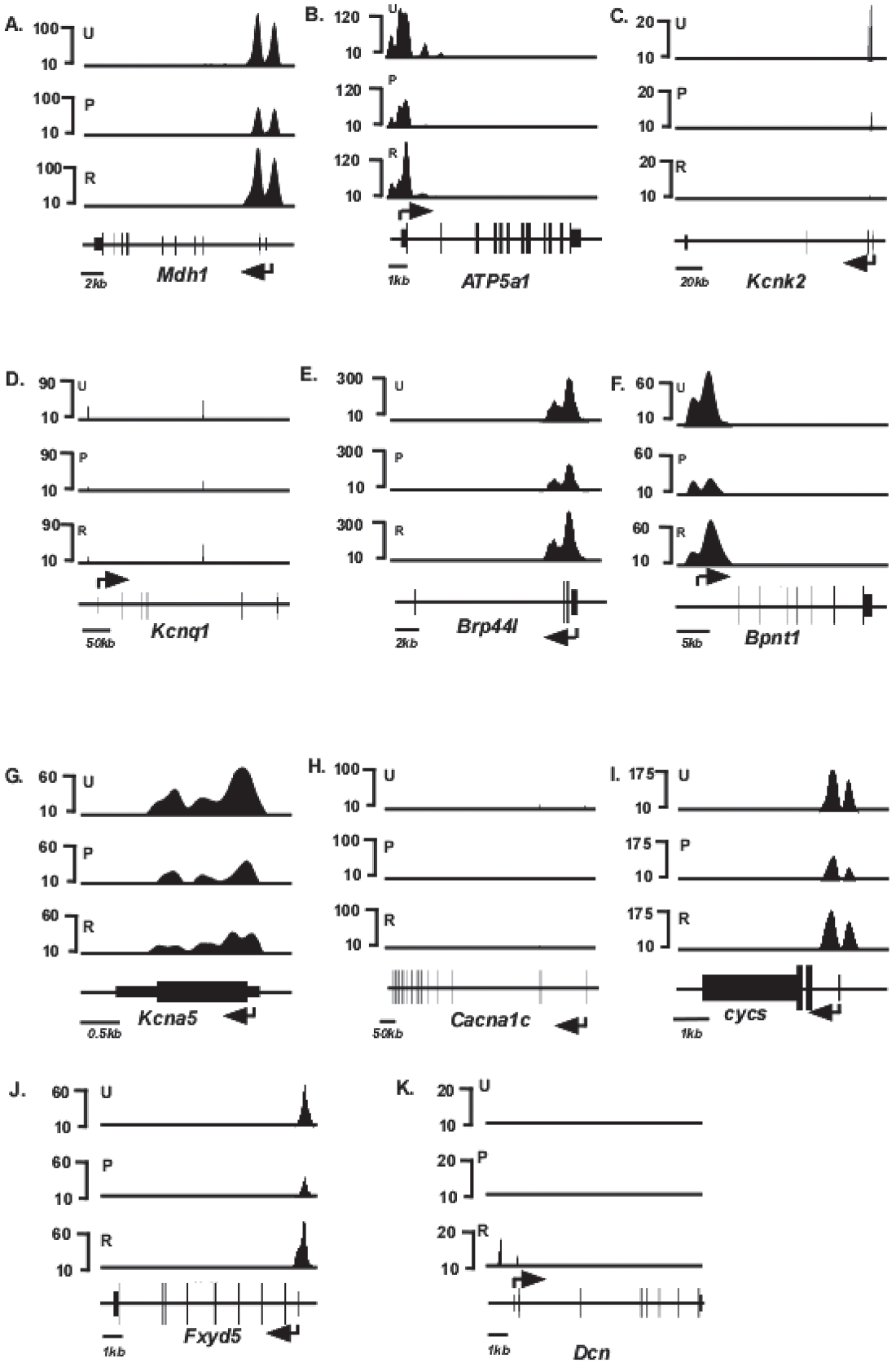

Figure 5. Schematic of H3K4me3 enrichment profile of T3-responsive genes that do not respond to PTU. Relative H3K4me3 signal intensities are shown on the *y*-axis and schematic of individual gene loci shown on the *x*-axis. ChIP-seq analyses were conducted using anti-H3K4me3 antibody from chromatin isolated from untreated (U, top panel), PTU-treated (P, middle panel), or reversal (R, bottom panel) animals. Exons are represented as closed boxes; bent arrows show the transcriptional start site (TSS) and direction of transcription. Quantitation of these data is presented in Tables 2 and 3. Scale bars for each locus are shown at the bottom left of each panel.

TABLE 2
CHANGES IN H3K4me3 LEVELS AMONG PUTATIVE T3-RESPONSIVE GENES

Gene Symbol	Ctl Levels	PTU Levels	Rev Levels	PTU/ Ctrl Ratio	Rev/ PTU Ratio
Myh6	68026	0	21573	0.0	—
Rgs4	2000	0	8942	0.0	—
Mgp	20267	602	42947	0.0	71.4
Pln	20090	1134	\N7021	0.1	6.2
Nppb	18315	2351	3857	0.1	1.6
Hr	18641	2638	7858	0.1	3.0
Kcnj11	34836	6006	0	0.2	0
Kcnd2	19304	3331	1535	0.2	0.5
Slc2a4	32417	6319	8694	0.2	1.4
Kcnb1	14129	2766	3523	0.2	1.3
Slc8a1	49337	11331	40608	0.2	3.6
Itga7	51115	14827	33826	0.3	2.3
Atp1b1	57529	16998	16922	0.3	1.6
Fabp3	95984	31582	44893	0.3	1.4
Atp2a2	84817	29090	47822	0.3	1.6
Ankrd1	17212	5936	3077	0.3	0.5
Cx3cl1	29320	10314	21145	0.4	2.1
Dab2	42588	17915	69258	0.4	3.9
Nrp1	171188	74166	179050	0.4	2.4
Mdh1	47128	22051	49320	0.5	2.2
Atp5a1	105564	49696	84171	0.5	1.7
Kcnk2	17021	8040	1352	0.5	0.2
Kcnq1	105988	50258	80012	0.5	1.6
Brp44l	101490	50152	88572	0.5	1.8
Bpnt1	74190	38480	57761	0.5	1.5
Kcna5	66864	35810	44242	0.5	1.2
Cacna1c	8782	4837	6618	0.6	1.4
Cycs	47220	28252	43321	0.6	1.5
Fxyd5	26130	17449	33009	0.7	1.9
Myh7	1160	12730	0	11.0	0
Actg2	ND	ND	ND	—	—
Aldoc	ND	ND	ND	—	—
Ctrb1	ND	ND	ND	—	—
Dcn	ND	ND	10456	—	—
Fbp1	ND	ND	ND	—	—
Kcne1	ND	ND	ND	—	—
Myh13	ND	ND	ND	—	—
Nppa	ND	ND	ND	—	—
S100a4	ND	ND	ND	—	—
Tmprss13	ND	ND	ND	—	—
Tnp2	ND	ND	ND	—	—
Wfdc8	ND	ND	ND	—	—

Quantification of H3K4me3 levels within putative T3-reponsive genes under untreated (Ctrl), PTU-treated (PTU), and reversal (Rev) conditions. ND, not detected. Changes in H3K4me3 levels were quantified based on values for ChIP-seq.

the H3K4me3 modification. The sites and levels of H3K4me3 modification were determined by massive parallel sequencing on an Illumina deep sequencing platform. Distribution patterns of H3K4me3 were quantified and graphically visualized with an integrated genome browser, which depicts H3K4me3 levels on the *y*-axis and the locus map for each gene on the *x*-axis.

Distribution of H3K4me3 Modification at the Myh Locus

Untreated Mice. We first analyzed the distribution of H3K4me3 in untreated animals, which express Myh6 at high levels and Myh7 at very low levels. The top panel (U, untreated) of Figure 1 illustrates the distribution pattern of H3K4me3 signals at the Myh loci. A schematic of the locus is shown at the bottom of the figure. Under untreated conditions, Myh6 shows two regions of H3K4me3 enrichment. One region lies within the Myh6 promoter [peak h, located at −1.0 kb relative to the transcription start site (TSS)]. The other region is located within the 5′ transcribed portion (peaks a through g in Fig. 1, between TSS and +8.5 kb relative to TSS) of Myh6 gene. The presence of these H3K4me3 modifications within Myh6 is consistent with the high level of expression of Myh6. Myh7, on the other hand, shows essentially undetectable H3K4me3 signals within the promoter and most of the transcribed portion of the gene in the untreated mice. This lack of H3K4me3 modification at Myh7 is consistent with the very low expression of Myh7 under untreated conditions. Interestingly, a region of H3K4me3 enrichment is found at the intergenic region between the two Myh genes, which is seen as multiple peaks (peaks i through n in Fig. 1) beginning at approximately 2.5kb upstream of Myh6 TSS and extending approximately 4 kb into the 3′ transcribed portion of Myh7 [illustrated in greater detail in Fig. 2, top panel (U)].

PTU-Treated Mice. To change the expression levels of the two Myh genes, we induced a hypothyroid condition by feeding mice a diet containing 0.15% PTU for 6 weeks. PTU is a specific inhibitor of thyroid hormone synthesis, and it has been well established that this level of PTU in the diet is sufficient to induce changes in the heart that are typical of hypothyroid conditions (15,22,26). PTU treatment dramatically silences Myh6 expression and substantially increases Myh7 gene expression (22,26). In our mice, mRNA analyses using real-time PCR from the PTU-treated and untreated hearts show, as expected, a substantial silencing of Myh6 (approximately 10-fold decrease) and a dramatic increase in Myh7 gene

TABLE 3
QUANTITATION OF H3K4me3 LEVELS AT VARIOUS REGIONS IN INDIVIDUAL GENES

Gene	Condition	Promoter	5′ UTR	First Intron	Other Introns	All Exons	3′ UTR
Myh6	Control	48029	19997	0	0	0	0
	PTU	0	0	0	0	0	0
	Reversal	14496	7077	0	0	0	0
Rgs4	Control	0	0	2000	0	0	0
	PTU	0	0	0	0	0	0
	Reversal	0	280	7806	0	857	0
Mgp	Control	0	568	13329	4456	1915	0
	PTU	0	0	521	0	81	0
	Reversal	0	451	29793	10286	2417	0
Pln	Control	0	8643	6843	0	1956	848
	PTU	0	567	567	0	0	0
	Reversal	0	3511	3511	0	0	0
Nppb	Control	0	646	2817	7903	6950	0
	PTU	0	248	0	0	2103	0
	Reversal	0	0	558	1344	1955	0
Hr	Control	5697	6496	822	211	5434	0
	PTU	0	1325	185	0	1128	0
	Reversal	0	3938	746	0	3174	0
Kcnj11	Control	0	2688	0	0	28240	3809
	PTU	0	355	0	0	3665	986
	Reversal	0	0	0	0	0	0
Kcnd2	Control	19304	0	0	0	0	0
	PTU	3331	0	0	0	0	0
	Revesal	1535	0	0	0	0	0
Slc2a4	Control	0	2239	20953	2367	6858	0
	PTU	0	1142	3625	0	1552	0
	Reversal	0	975	6325	0	1395	0
Kcnb1	Control	12711	709	0	0	709	0
	PTU	2231	268	0	0	268	0
	Reversal	2523	0	0	0	0	0
Slc8a1	Control	0	24675	24293	0	369	0
	PTU	0	5665	5665	0	0	0
	Reversal	0	20304	20304	0	0	0
Itga7	Control	0	2936	36801	0	11378	0
	PTU	0	364	11509	0	2954	0
	Reversal	0	2067	22184	0	9575	0
Atp1b1	Control	0	7670	37385	0	12474	0
	PTU	0	2245	10793	0	3959	0
	Reversal	0	1765	20615	0	4543	0
Fabp3	Control	4334	0	37385	0	2997	0
	PTU	0	0	1073	0	1083	0
	Reversal	0	0	20615	0	1320	0
Atp2a2	Control	0	11767	30530	20653	20866	0
	PTU	0	5172	14109	0	9808	0
	Reversal	0	1002	22140	19106	5575	0
Ankrd1	Control	0	0	5317	6689	5206	0
	PTU	0	0	1614	1416	2906	0
	Reversal	0	0	1527	0	1550	0
Cx3cl1	Control	0	1848	21708	0	5764	0
	PTU	0	505	8164	0	1644	0
	Reversal	0	1046	16856	0	3243	0

(*continued*)

TABLE 3
CONTINUED

Gene	Condition	Promoter	5′ UTR	First Intron	Other Introns	All Exons	3′ UTR
Dab2	Control	0	21308	18574	0	2706	0
	PTU	0	8964	7828	0	1123	0
	Reversal	0	34650	31026	0	3581	0
Nrp1	Control	41277	13383	92480	2449	21600	0
	PTU	20895	7504	34309	0	11458	0
	Reversal	31449	13472	111118	637	22375	0
Mdh1	Control	0	4922	37028	0	5179	0
	PTU	0	3587	14715	0	3750	0
	Reversal	0	3735	35533	0	7051	0
Atp5a1	Control	0	6115	79019	7882	12548	0
	PTU	0	3650	39448	0	6598	0
	Revesal	0	4569	68859	2682	8061	0
Kcnk2	Control	0	0	7909	0	596	8517
	PTU	0	0	3356	0	658	4026
	Reversal	0	0	676	0	0	676
Kcnq1	Control	0	1330	16363	76913	11382	0
	PTU	0	470	8176	35882	5731	0
	Reversal	0	276	2575	71598	5563	0
Brp44I	Control	3623	1955	88258	0	7654	0
	PTU	547	944	44962	0	3699	0
	Reversal	2989	2044	76059	0	7522	0
Bpnt1	Control	53583	10332	7823	0	2452	0
	PTU	28490	5006	4043	0	941	0
	Reversal	34568	10117	8414	0	1662	0
Kcna5	Control	0	4902	0	0	60396	1566
	PTU	0	2298	0	0	33471	41
	Reversal	0	3248	0	0	39730	1264
Cacna1c	Control	3540	5242	0	0	0	0
	PTU	1976	2861	0	0	0	0
	Reversal	2456	4162	0	0	0	0
Cycs	Control	0	23373	21723	0	2124	0
	PTU	0	14144	13296	0	813	0
	Reversal	0	21429	20621	0	1272	0
Fxyd5	Control	0	12495	9107	476	4051	0
	PTU	0	7831	5846	1067	2706	0
	Reversal	0	14289	11825	3119	3776	0
Myh7	Control	0	0	0	0	0	1160
	PTU	0	0	12730	0	0	0
	Reversal	0	0	0	0	0	0
Actg2	Control	0	0	0	0	0	0
	PTU	0	0	0	0	0	0
	Reversal	0	0	0	0	0	0
Aldoc	Control	0	0	0	0	0	0
	PTU	0	0	0	0	0	0
	Reversal	0	0	0	0	0	0
Ctrb1	Control	0	0	0	0	0	0
	PTU	0	0	0	0	0	0
	Reversal	0	0	0	0	0	0
Dcn	Control	0	0	0	0	0	0
	PTU	0	0	0	0	0	0
	Reversal	7907	0	1279	108	1161	0

TABLE 3
CONTINUED

Gene	Condition	Promoter	5′ UTR	First Intron	Other Introns	All Exons	3′ UTR
Fbp1	Control	0	0	0	0	0	0
	PTU	0	0	0	0	0	0
	Reversal	0	0	0	0	0	0
Kcne1	Control	0	0	0	0	0	0
	PTU	0	0	0	0	0	0
	Reversal	0	0	0	0	0	0
Myh13	Control	0	0	0	0	0	0
	PTU	0	0	0	0	0	0
	Reversal	0	0	0	0	0	0
Nppa	Control	0	0	0	0	0	0
	PTU	0	0	0	0	0	0
	Reversal	0	0	0	0	0	0
S100a4	Control	0	0	0	0	0	0
	PTU	0	0	0	0	0	0
	Reversal	0	0	0	0	0	0
Tmprss13	Control	0	0	0	0	0	0
	PTU	0	0	0	0	0	0
	Reversal	0	0	0	0	0	0
Tnp2	Control	0	0	0	0	0	0
	PTU	0	0	0	0	0	0
	Reversal	0	0	0	0	0	0
Wfdc8	Control	0	0	0	0	0	0
	PTU	0	0	0	0	0	0
	Reversal	0	0	0	0	0	0

Quantification of H3K4me3 levels at different regions within putative T3-reponsive genes under untreated (Ctrl), PTU-treated (PTU), and reversal (Rev) conditions. ND, not detected. Changes in H3K4me3 levels were quantified based on values for ChIP-seq.

expression (approximately 50-fold increase) in response to PTU (Fig. 3). The middle section (P) of Figure 1 illustrates the H3K4me3 distribution under PTU-treated conditions. At the Myh6 locus this treatment leads to a dramatic decrease of the H3K4me3 signals to undetectable levels (reduction to <20% of its maximal value, a level below which random noise predominates) at the two regions of the gene that showed high levels of H3K4me3 modification in the untreated mice (peaks a through n in Fig. 1). This loss of H3K4me3 modification is consistent with the greatly reduced level of gene expression. At the Myh7 locus, PTU treatment causes the development of two new peaks of H3K4me3 enrichment. One peak is at +0.5 kb (peak p in Fig. 1) and the other peak is located at +2.5kb (peak o in Fig. 1) relative to the Myh7 TSS. This gain of H3K4me3 modification is consistent with the greatly increased expression levels of Myh7. There are, however, no H3K4me3 peaks present within the Myh7 promoter, confirming our previous observation that H3K4me3 modifications are absent at the Myh7 promoter when it is expressed in the adult heart under hypothyroid condition (20). The intergenic region, noted above, completely loses the H3K4me3 signals during PTU treatment (note absence of peaks i though n in panel P, Figs. 1 and 2).

Reversal Mice. We next determined the degree to which the PTU-induced changes in H3K4me3 distribution at the Myh locus reverse when the gene expression levels are reversed, which our previous work shows is complete by 2 weeks after withdrawal of PTU. Accordingly, mice were treated with PTU for 6 weeks, PTU treatment was then withdrawn, and 2 weeks later we sacrificed the mice. Real-time PCR analyses for mRNA expression show that Myh6 gene expression returns to its original high levels, while expression of Myh7 is reduced dramatically to its original low levels (Fig. 3). ChIP-seq analyses conducted on the hearts of these animals show that the PTU-induced changes in H3K4me3 enrichment within the Myh7 gene have likewise returned to the

untreated levels. Thus, as illustrated in bottom panel (R) of Fig. 1, the two H3K4me3 peaks (peaks o and p) present at Myh7 gene under PTU conditions decrease dramatically during reversal to levels below the threshold and so indistinguishable from those of untreated animals. The Myh6 gene shows increases in the H3K4me3 levels within the 5′ transcribed portion during reversal, but neither the levels nor the patterns are restored to their untreated levels. The peaks a, b, and c present in the 5′ transcribed region are not reattained during reversal conditions. Nor is the peak in the promoter (peak h) reattained under reversal conditions. The heights of the H3K4me3 modification within the 5′ transcribed portion were also reduced under reversal condition compared with the untreated condition (compare peaks e, f, and g with peaks e′, f′, and g′, respectively, in Fig,. 1). The intergenic region also shows increases in the levels of H3K4me3 modification. However, similar to the situation for Myh6, some peaks (peaks i, m, and n in Figs. 1 and 2) are not reattained, and some peaks show decreased heights (compare peaks j, k, and l

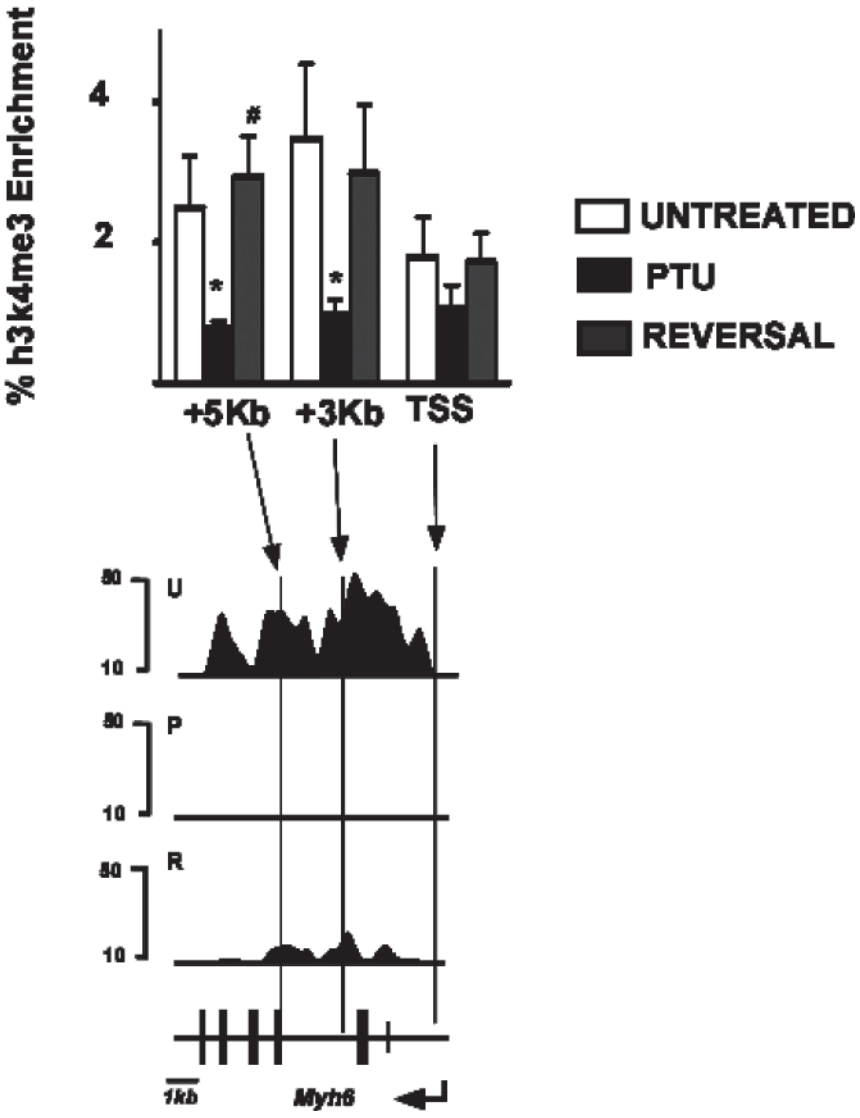

Figure 6. Validation of ChIP-seq data. Top: ChIP-qPCR analyses for H3K4me3 at the Myh6 transcribed region. % enrichment (relative to 100% input) of immunoprecipitated DNA is shown on *y*-axis and the various locations (TSS, transcription start site, +3 kb, +5 kb) of Myh6 are shown on the *x*-axis. ChIP-qPCRs were conducted using anti-H3K4me3 antibody form chromatin isolated from untreated (U, open bars), PTU-treated (P, black bars), or reversal (R, gray bars) animals. Data represent mean of seven independent ChIP experiments from four individual animals within each group. Error bars represent SEM. $*p < 0.05$ (relative to untreated group), $\#p < 0.005$ (relative to PTU group). These data are reproduced from a previously published work (20). Bottom: Chip-seq analyses of Myh6 gene. Part of Figure 1 is shown below the graph for ease of comparison. Scale bar for the locus is shown at the bottom left.

TABLE 4
CHANGES IN mRNA LEVELS AMONG PUTATIVE T3-RESPONSIVE GENES

Gene Symbol	PTU/Ctrl Ratio	Rev/PTU Ratio
Tmprss13	0.2	2.6
Hr	0.3	2.5
Myh6	0.3	3.1
Rgs4	0.4	2.5
Kcnb1	0.5	2.9
Kcnq1	2.1	0.4
Kcne1	3.6	0.4
Myh7	3.0	0.1
Actg2	—	—
Atp2a2	—	—
Atp5a1	—	—
Bpnt1	—	—
Cx3cl1	—	—
Cycs	—	—
Dab2	—	—
Dcn	—	—
Fabp3	—	—
Fxyd5	—	—
Itga7	—	—
Kcna5	—	—
Kcnd2	—	—
Kcnj11	—	—
Mdh1	—	—
Mgp	—	—
Nppa	—	—
Nppb	—	—
Nrp1	—	—
Pln	—	—
S100a4	—	—
Slc2a4	—	—
Slc8a1	—	—
Aldoc	ND	ND
Ankrd1	ND	ND
Atp1b1	ND	ND
Brp44l	ND	ND
Cacna1c	ND	ND
Ctrb1	ND	ND
Fbp1	ND	ND
Kcnk2	ND	ND
Myh13	ND	ND
Tnp2	ND	ND
Wfdc8	ND	ND

Changes in mRNA levels of putative T3-reponsive genes under untreated (Ctrl), PTU-treated (PTU), and reversal (Rev) conditions. Genes whose expression changed <2× are denoted by —. ND, not detected. Changes in mRNA levels were quantified based on microarray analyses.

with peaks j′, k′, and l′, respectively, in Figs. 1 and 2). Thus, reversal of gene expression of Myh genes to untreated levels results in a full reversal of H3K4me3 modification at the Myh7 gene, but that at the Myh6 gene is only partial.

Distribution of H3K4me3 Modification in Other T3-Responsive Genes

Forty genes, in addition to Myh6 and Myh7, have been shown by previous investigators to be responsive to T3 (1,15) (Table 1). Inspection of the H3K4me3 distribution patterns of these 40 genes in the untreated mice show that 28 have detectable H3K4me3 modifications indicative of expression [top panel (U) of Figs. 4 and 5] These H3K4me3 peaks are distributed primarily at the 5′ transcribed portions of these genes, as has been observed for other actively transcribed genes. PTU treatment changed the level of H3K4me3 modification significantly (defined as >2× changes in H3K4me3 levels in either direction) in 18 of these genes [middle panel (P) of Fig. 4], while the remaining 10 genes did not show a significant PTU-response [middle panel (P) of Fig. 5]. Under conditions of reversal, H3K4me3 levels within these 18 genes had a tendency to return to the original untreated conditions [bottom panel (R) of Fig. 4], although the levels did not always show full recovery. Six genes (Kcnj11, Hr, Pln, Nppb, Slc2a4, and Ankrd1) do not show full recovery. Kcnj11 loci shows dramatically reduced H3K4me3 levels under reversal conditions, compared to untreated conditions (Fig. 4F), while the H3K4me3 peaks present in the promoter of Hr and Slc2a4 (arrows, Fig. 4E and H, respectively), 5′ transcribed portion of Pln (arrows, Fig. 4C), and within the gene of Nppb and Anrd1 (arrows, Fig. 4D and O, respectively) are not reattained under reversal conditions. Interestingly, one gene (Dcn) that had previously showed undetected levels of H3K4me3 under untreated and PTU conditions shows detectable levels of H3K4me3 levels under conditions of reversal (Fig. 5K). Quantified values of H3K4me3 levels at the entire loci of all these genes are shown in Table 2, and the distributions within various regions of individual genes are shown in Table 3.

We compared the ChIP-seq data for Myh6 described in this work with ChIP-qPCR analyses of Myh6 carried out previously by us (20) in response to PTU treatment and PTU reversal. The previous ChIP-qPCR analyses showed that the +3 kb and +5 kb regions of Myh6 gene had significant reversible decreases in H3K4me3 signals in response to PTU treatment (Fig. 6, black bars), while the TSS region of Myh6 gene showed no changes in H3K4me3 levels in response to these treatments. These ChIP-qPCR data are in complete agreement with the ChIP-seq data for Myh6 at these locations presented in this report (Fig. 6, bottom panel).

We also examined whether the T3-responsive genes that showed changes in H3K4me3 levels also showed changes in gene expression. To do this, we conducted microarray analyses from hearts of mice from the three groups, and the results are shown in Table 4. Eight out of 42 genes show significant changes in mRNA levels (determined as >2× change

in either direction). Six of these genes (Myh6, Rgs4, Hr, Kcnb1, Kcnq1, and Myh7) also showed changes in H3K4me3 levels, while two genes (Tmprss13 and Kcne1) did not show any detectable H3K4me3 signals at their respective loci.

DISCUSSION

The ChIP-seq procedure combines chromatin immunoprecipitation with high-throughput direct sequencing of short fragments of DNA (19,31). The method is devoid of sequence bias and has great sensitivity and consequently provides a way of mapping a wide variety of histone modifications across the whole genome (10,23). In this study we have applied this procedure to investigate the distribution of H3K4me3 marks at the Myh locus in response to reversible changes in gene expression triggered by chemical inhibition of T3 synthesis.

Our ChIP-seq analyses show a correlation between H3K4me3 signals and the gene expression status of Myh6 and Myh7 genes. When Myh6 gene expression is high, as under untreated and reversal conditions, we find detectable levels of H3K4me3 at the Myh6 locus. Similarly, when Myh7 gene expression is high, as under conditions of PTU treatment, we find detectable levels of H3K4me3 modifications at the Myh7 locus. When Myh6 gene expression is silenced, as under conditions of PTU treatment, H3K4me3 levels also drops to low levels at the Myh6 locus. Similarly, when Myh7 gene expression is silenced, under untreated and reversal conditions, H3K4me3 modifications likewise drop to low levels.

Our previous work using ChIP-qPCR showed that the promoter of Myh7 did not show detectable changes in H3K4me3 modifications in response to PTU-induced changes in gene expression (20). Consistent with these previous ChIP-qPCR data, our current ChIP-seq data do not show PTU-induced changes in the levels of H3K4me3 levels in the promoter region of Myh7. Rather, the distribution of this modification occurs at a region downstream of the TSS. Thus, our new ChIP-seq data imply that if H3K4me3 modifications play a role in the expression of the Myh7 gene, it is not by changing the modification levels in the promoter region. The significance of the differences in H3K4me3 modification at the two Myh promoters remains to be determined.

Interestingly, our data show the presence of a region of H3K4me3 modification in the intergenic region between Myh6 and Myh7 under untreated conditions, beginning approximately 2.5 kb upstream of Myh6 TSS and extending for 6.5 kb into the 3′ region of Myh7. This observation is a strong indicator that there is transcriptional activity in this intergenic region of the cardiac MHC locus, in confirmation of several previous reports demonstrating the presence of an antisense intergenic promoter at this location (4,5,7,9). This antisense promoter is thought to direct a transcript across the Myh7 gene and may play a role in controlling the switch between Myh6 and Myh7 gene expression. Multiple binding sites for the THR are present within this intergenic region, and previous work suggests that this promoter is under the control of T3, and has documented the presence of a PTU-responsive change in the levels of h3k9/14 ac and h3k4/k9 me3 at this intergenic promoter (8). Consistent with this our data show that PTU treatment leads to a dramatic reduction of H3K4me3 modification in this region, which is reversed when the PTU treatment is ceased, and the intergenic changes correlates with changes occurring within the Myh6 gene. Together, these observations of T3-mediated epigenetic changes in H3K4me3 signals at this location make a strong case for the presence of a functional antisense promoter in this intergenic region.

Our analyses demonstrate that 18 other putative T3-responsive genes show very modest changes in H3K4me3 levels in response to PTU. All of these are reductions in the levels of H3K4me3, consistent with previous observations that the vast majority of T3-responsive genes are positively regulated by T3. Since cardiac myocytes do not divide in the adult mouse heart to any appreciable degree, any decreases in H3K4me3 levels must be a direct result of active removal of the modification via demethylase rather than being the result of dilution due to cell division.

Even though Myh6 gene expression levels fully returned to their original state, the H3K4me3 modification within the Myh6 locus only partially returned to the original state. Thus, some peaks that were present under untreated conditions were absent under reversal conditions, while other peaks had a marked decrease in amplitude, although the expression levels were comparable between the two conditions. The achievement of full restoration of Myh6 gene expression, even though the H3K4me3 pattern is only partially restored, shows that full reexpression of Myh6 does not require that the H3K4me3 modifications return fully to the untreated conditions. The degree of reversal also varied at the non-Myh loci. Thus, one gene (Kcnj11) showed no reversal while five genes (Hr, Pln, Nppb, Slc2a4, and Ankrd1) showed partial reversal of the H3K4me3 distribution when PTU was withdrawn. Since each nucleosome contains two h3 molecules, a single nucleosome can have at least three discrete H3K4me3 modification states: zero (both h3k4 unmodified), one (only one H3K4me3 modified), or two (both h3k4 modified). The partial H3K4me3 levels seen at a particular position may

represent either partial modification of all nucleosomes at that position, full modification of a fraction of DNA molecules in the population, or a combination of both. More work is required to distinguish between these various possibilities.

Our results also demonstrate that genes that show changes in mRNA levels, in general, also show changes in H3K4me3 levels but not vice versa. Thus, 75% (6/8) of genes that showed changes in mRNA levels showed changes in H3K4me3 levels, but only 30% (6/20) genes that showed changes in H3K4me3 levels also showed changes in mRNA levels. It is possible that the two genes that showed changes in mRNA levels in absence of H4K4me3 may be regulated in a posttranscriptional manner, which generally does not involve changes in histone modifications. It has also been demonstrated that some genes show changes in H3K4me3 levels in the absence of changes in mRNA levels—a phenomenon termed "poised"—as a prelude to subsequent increases in transcription. It is possible that several of the 14 genes that showed changes in H3K4me3 levels in the absence of changes in mRNA levels may belong to this category.

ACKNOWLEDGMENTS

The work was supported by grants from NIH (HL49277), Grant-in-Aid for Scientific Research (B) 22310117, Grant-in-Aid for Exploratory Research 23659050, from the Japan Society for the Promotion of Science, and Grant-in-Aid for Scientific Research on Innovative Areas 23125503 from the Ministry of Education, Culture, Sports, Science and Technology, Japan. We would like to thank Akashi Izumi and Kaori Shiina for Solexa sequencing, and Hiroshi Kimura for monoclonal antibody for H3K4me3, and Feng Li for the critical reading of the manuscript.

REFERENCES

1. Adamson, C.; Maitra, N.; Bahl, J.; Greer, K.; Klewer, S.; Hoying, J.; Morkin, E. Regulation of gene expression in cardiomyocytes by thyroid hormone and thyroid hormone analogs 3,5-diiodothyropropionic acid and CGS 23425 [N-[3,5-dimethyl-4-(4′-hydroxy-3′-isopropylphenoxy)-phenyl]-oxamic acid]. J. Pharmacol. Exp. Ther. 311:164–171; 2004.
2. Aranda, A.; Pascual, A. Nuclear hormone receptors and gene expression. Physiol. Rev. 81:1269–1304; 2001.
3. Dillmann, W. H. Cellular action of thyroid hormone on the heart. Thyroid 12: 447–452; 2002.
4. Giger, J.; Qin, A. X.; Bodell, P. W.; Baldwin, K. M.; Haddad, F. Activity of the beta-myosin heavy chain antisense promoter responds to diabetes and hypothyroidism. Am. J. Physiol. Heart Circ. Physiol. 292: H3065–3071; 2007.
5. Giger, J. M.; Bodell, P. W.; Baldwin, K. M.; Haddad, F. The CAAT-binding transcription factor 1/nuclear factor 1 binding site is important in beta-myosin heavy chain antisense promoter regulation in rats. Exp. Physiol. 94:1163–1173; 2009.
6. Guenther, M. G.; Levine, S. S.; Boyer, L. A.; Jaenisch, R.; Young, R. A. A chromatin landmark and transcription initiation at most promoters in human cells. Cell 130:77–88; 2007.
7. Haddad, F.; Bodell, P. W.; Qin, A. X.; Giger, J. M.; Baldwin, K. M. Role of antisense RNA in coordinating cardiac myosin heavy chain gene switching. J. Biol. Chem. 278:37132–37138; 2003.
8. Haddad, F.; Jiang, W.; Bodell, P. W.; Qin, A. X.; Baldwin, K. M. Cardiac myosin heavy chain gene regulation by thyroid hormone involves altered histone modifications. Am. J. Physiol. Heart Circ. Physiol. 299:H1968–1980; 2010.
9. Haddad, F.; Qin, A. X.; Bodell, P. W.; Zhang, L. Y.; Guo, H.; Giger, J. M.; Baldwin, K. M. Regulation of antisense RNA expression during cardiac MHC gene switching in response to pressure overload. Am. J. Physiol. Heart Circ. Physiol. 290:H2351–2361; 2006.
10. Ishihara, K.; Oshimura, M.; Nakao, M. CTCF-dependent chromatin insulator is linked to epigenetic remodeling. Mol. Cell 23:733–42; 2006.
11. Kahaly, G. J.; Dillmann, W. H. Thyroid hormone action in the heart. Endocr. Rev. 26:704–728; 2005.
12. Kim, J.; Daniel, J.; Espejo, A.; Lake, A.; Krishna, M.; Xia, L.; Zhang, Y.; Bedford, M. T. Tudor, MBT and chromo domains gauge the degree of lysine methylation. EMBO Rep. 7:397–403; 2006.
13. Kimura, H.; Hayashi-Takanaka, Y.; Goto, Y.; Takizawa, N.; Nozaki, N. The organization of histone H3 modifications as revealed by a panel of specific monoclonal antibodies. Cell Struct. Funct. 33:61–73; 2008.
14. Kouzarides, T. Chromatin modifications and their function. Cell 12:693–705; 2007.
15. Le Bouter, S.; Demolombe, S.; Chambellan, A.; Bellocq, C.; Aimond, F.; Toumaniantz, G.; Lande, G.; Siavoshian, S.; Baro, I.; Pond, A. L.; Nerbonne, J. M.; Leger, J. J.; Escande, D.; Charpentier, F. Microarray analysis reveals complex remodeling of cardiac ion channel expression with altered thyroid status relation to cellular and integrated electrophysiology. Circ. Res. 92: 234–242; 2003.
16. Lee, B. M.; Mahadevan, L. C. Stability of histone modifications across mammalian genomes implications for 'epigenetic' marking. J. Cell. Biochem. 108:22–34; 2009.
17. Li, B.; Carey, M.; Workman, J. L. The role of chromatin during transcription. Cell 128:707–719; 2007.
18. Mellor, J.; Dudek, P.; Clynes, D. A glimpse into the epigenetic landscape of gene regulation. Curr. Opin. Genet. Dev. 18:116–122; 2008.

19. Mendenhall, E. M.; Bernstein, B. E. Chromatin state maps new technologies, new insights. Curr. Opin. Genet. Dev. 18:109–115; 2008.
20. Pandya, K.; Pulli, B.; Bultman, S.; Smithies, O. Reversible epigenetic modifications of the two cardiac myosin heavy chain genes during changes in expression. Gene Expr. 15:51–59; 2011.
21. Portman, M. A. Thyroid hormone regulation of heart metabolism. Thyroid 18:217–225; 2008.
22. Rundell, V. L.; Manaves, V.; Martin, A. F.; de Tombe, P. P. Impact of beta-myosin heavy chain isoform expression on cross-bridge cycling kinetics. Am. J. Physiol. Heart Circ. Physiol. 288:H896–903; 2005.
23. Saitoh, N.; Bell, A. C.; Recillas-Targa, F.; West, A. G.; Simpson, M.; Pikaart, M.; Felsenfeld, G. Structural and functional conservation at the boundaries of the chicken beta-globin domain. EMBO J. 19:2315–2322; 2000.
24. Santos-Rosa, H.; Schneider, R.; Bannister, A. J.; Sherriff, J.; Bernstein, B. E.; Emre, N. C.; Schreiber, S. L.; Mellor, J.; Kouzarides, T. Active genes are tri-methylated at K4 of histone H3. Nature 419:407–411; 2002.
25. Seila, A. C.; Calabrese, J. M.; Levine, S. S.; Yeo, G. W.; Rahl, P. B.; Flynn, R. A.; Young, R. A.; Sharp, P. A. Divergent transcription from active promoters. Science 322:1849–1851; 2008.
26. van Rooij, E.; Sutherland, L. B.; Qi, X.; Richardson, J. A.; Hill, J.; Olson, E. N. Control of stress-dependent cardiac growth and gene expression by a microRNA. Science 316:575–579; 2007.
27. Wada, H.; Hashimoto, K.; Wada, Y.; Kobayashi, M.; Izumi, A.; Sugiyama, A.; Kohro, T.; Hamakubo, T.; Kodama, T. Extensive oligonucleotide microarray transcriptome analysis of the rat cerebral artery and arachnoid tissue. J. Atheroscler. Thromb. 9:224–232; 2002.
28. Wada, Y.; Ohta, Y.; Xu, M.; Tsutsumi, S.; Minami, T.; Inoue, K.; Komura, D.; Kitakami, J.; Oshida, N.; Papantonis, A.; Izumi, A.; Kobayashi, M.; Meguro, H.; Kanki, Y.; Mimura, I.; Yamamoto, K.; Mataki, C.; Hamakubo, T.; Shirahige, K.; Aburatani, H.; Kimura, H.; Kodama, T.; Cook, P. R.; Ihara, S. A wave of nascent transcription on activated human genes. Proc. Natl. Acad. Sci. USA 106:18357–18361; 2009.
29. Wang, Z.; Zang, C.; Rosenfeld, J. A.; Schones, D. E.; Barski, A.; Cuddapah, S.; Cui, K.; Roh, T. Y.; Peng, W.; Zhang, M. Q.; Zhao, K. Combinatorial patterns of histone acetylations and methylations in the human genome. Nat. Genet. 40:897–903; 2008.
30. Yen, P. M. Physiological and molecular basis of thyroid hormone action. Physiol. Rev. 81:1097–1142; 2001.
31. Zecchini, V.; Mills, I. G. Putting chromatin immunoprecipitation into context. J. Cell. Biochem. 107:19–29; 2009.